Geophys. J. R. astr. Soc. (1975) **42**, 977–991

Joint Inversion of Geophysical Data

K. Vozoff and D. L. B. Jupp

(Received 1974 September 26)

Summary

By jointly inverting several different kinds of geophysical measurements at a site we avoid some of the ambiguity inherent in the individual methods. We show how this can be done for the combination of DC resistivity and magnetotelluric measurements on a layered medium by considering a simple 3-layer model. The combination resolves the resistivity of the thin resistive second layer, even though neither of the two methods can do so alone.

The method is then applied to field data from a shallow sedimentary basin. A blind zone occurs beneath a thick near-surface conductive shale. By a study of the eigenvalue structure of the model it can be seen that resolution in this zone would be slightly enhanced by higher frequency magnetotelluric data, but additional DC data at larger spacing would yield no improvement.

Introduction

Inversion of geophysical data consists of operating directly on those data so as to generate a view of the structure which causes them. It differs from the traditional forward approach to geophysical interpretation in which a model is assumed, its response is calculated and compared with the observations, and the model parameters are then modified in a way which will hopefully improve the comparison. The virtues of inversion, if it has any, are that it uses the data to the fullest while being more economical of skilled interpreter time than is the forward approach. Consideration of the interpretation problem also suggests that it will sometimes be more cost-effective to acquire a limited number of measurements of several types than many measurements of a single type, in development and exploration programs.

The recent geophysical literature includes many works on development and application of inversion techniques. It is a topic of widespread active research. Most applied papers have dealt with seismic properties of the Earth, although some have treated electromagnetic properties (Parker 1970) and localized exploration-scale problems (Inman, Ryu & Ward 1973).

We treat here the problem of joint inversion of two related kinds of data, DC resistivity and Ultra Low Frequency electromagnetic (magnetotelliric) measurements in horizontally-layered conditions. The approach is outlined and examples are presented in which the combination yields more satisfactory results than either of the two methods does alone.

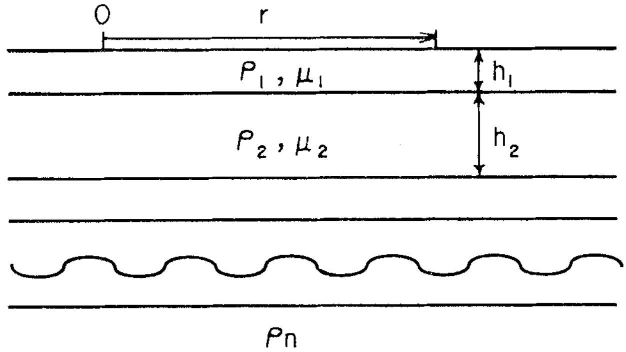

FIG. 1 The general horizontal layer model.

The two forward problems

Theory for both the DC resistivity (DC) and the Magnetotelluric (MT) methods in layered media is well known (e.g. see Ward, 1967, pages 93, 117). That is, given a model containing a number of layers, their thicknesses, and their electromagnetic properties (Fig. 1), it is a nearly trivial exercise to calculate model responses to the two methods. The analytic expressions for these responses are tabulated in Table 1.

Analysis of the two sets of equations illustrates the characteristics of each which makes them complementary to some extent It is well known that the MT method has poor sensitivity to resistive layers: a thin resistive layer is ignored whereas response of a thick resistive layer depends only on its thickness and not on its resistivity. MT is highly responsive to conductive layers even if they are very thin. DC on the other hand is virtually unbiased in the responses (Fig. 2), but for thin layers these depend only on the product of conductivity-thickness (conductive layers) or resistivity-

Table 1

DC (point source of current I at $r=0$)	MT (plane wave)
$\rho_a(r) = \frac{I}{2\pi} \int_0^\infty k_1(\lambda)\, J_0(\lambda r)\, d\lambda$	$\rho_a(\omega) = \frac{1}{\lvert w \rvert^2} Z_1{}^* Z_1$
$k_1(\lambda) = \frac{k_2 + T_1}{S_1 k_2 + 1}$	$\phi(\omega) = \arctan \frac{\mathrm{Im}\,[Z]}{\mathrm{Re}\,[Z]}$
$k_i(\lambda) = \frac{k_{i+1} + T_i}{S_i k_{i+1} + 1}$	$Z_i(\omega) = \frac{Z_{i+1} + T_i}{S_i Z_{i+1} + 1}$
$T_i = \rho_i \tanh(\lambda h_i)$	$T_i = w\sqrt{(\rho_i)} \tanh(w h_i/\sqrt{\rho_i})$
$S_i = \frac{1}{\rho_i} \tanh(\lambda h_i)$	$w = \sqrt{(-i\omega\mu)}$
$k_n = \rho_n$	$S_i = \frac{1}{w\sqrt{\rho_i}} \tanh(w h_i/\sqrt{\rho_i})$
$J_0(x)$ = Bessel function	$Z_n = w\sqrt{\rho_n}$

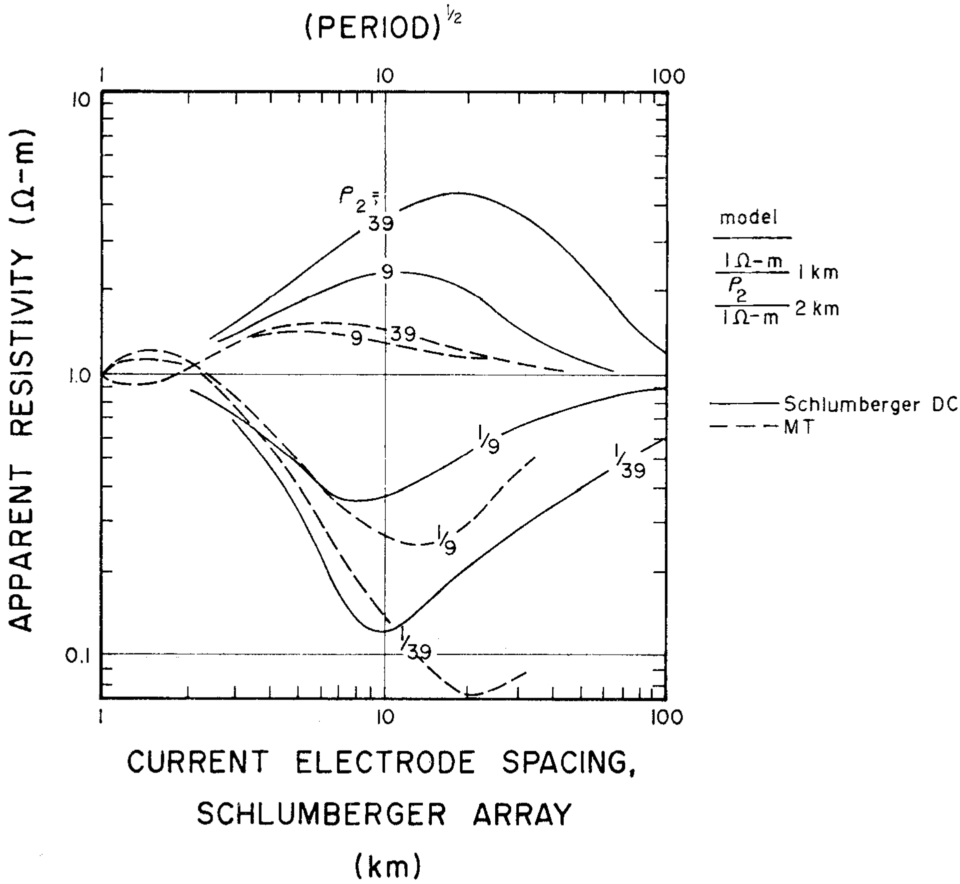

FIG. 2 Responses of the DC resistivity and MT methods to the 3-layer model shown.

thickness (resistive layers). DC has poor resolution in the case of models containing layers of highly-contrasting properties.

The two methods are complementary in another sense. For practical reasons it is easy and inexpensive to obtain DC data relating to shallow depths (less than a few kilometres), but difficult to obtain deeper DC data. Just the reverse is true of MT. Low frequency MT information which refers to depths beyond a few kilometres is normally more easily obtained than it is at higher frequencies. Yet MT data are better interpreted with a knowledge of shallow conditions. In the examples which follow we demonstrate some advantages of a stereoscopic approach to interpretation.

Formulating and solving the joint problem

Our approach to inversion is set out in the accompanying paper ' Stable Iterative Methods for the Inversion of Geophysical Data ' subsequently referenced as SIM (Jupp & Vozoff, 1975).

For general joint inversion problems, the proper combination of the two data sets, and weighting of the influence of the same earth model on the different responses, is very important.

For isotropic, horizontally layered earth models, the MT data and DC data measure 'earth' response to two distinct inputs through quite distinct physical processes. However, the output apparent resistivities have very similar features. For example, at long (DC) spacings and long (MT) periods, both are asymptotic to basement resistivity ρ_N. For short spacings and short periods, both are asymptotic to ρ_1.

When the data are not from an (approximately) layered situation, of course, the joint process cannot be expected to improve their interpretation. A more complex model, together with joint inversion, is needed for this case. In SIM we describe how an iterative method, based on the Gauss iterative method (Kowalik & Osborne 1968), may be used to solve inverse problems, wherein data are fitted to a layered (or some other more complex but nevertheless simplified) earth model. The approach is to evaluate the forward problem to determine how well a current earth model fits the data, and to evaluate the 'parameter influence' (or Jacobian, or partials) matrix to determine how the model should be altered to improve the fit.

The 'parameter influence' matrix

$$J = [J_{ij}]_{\substack{i=1,M \\ j=1,N}}$$

has components

$$J_{ij} = w_i \frac{\partial g_i}{\partial x_i} \text{ (where } w_i \text{ indicates relative importance of observation } i\text{)}$$

which is the variation of the i'th data value, with respect to changes in the j'th parameter (layer resistivity, or thickness). That is, it measures the influence of changes in parameters on the (model predicted) data.

To properly combine the separate DC and MT problems in an inversion method, the separate influence matrices need to be balanced. In our problems, since the layer resistivities and thicknesses have implicit constraints

$$\begin{cases} \rho_i \geqslant 0 & i = 1, \overline{N+1} \\ h_i \geqslant 0 & i = 1, N \end{cases}$$

we may force the constraints by letting

$$x_j = \log \rho_j \text{ for } j = 1, \overline{N+1}$$

$$x_{j+N+1} = \log h_j \text{ for } j = 1, N.$$

If, moreover, we use relative errors, the elements of the influence matrix take the form

$$J_{ij} = w_i \frac{\partial g_i}{\partial x_j} = \frac{1}{g_i} \frac{\partial g_i}{\partial \log \rho_j} = \frac{\rho_j}{g_i} \frac{\partial g_i}{\partial \rho_j}$$

$$\text{or} \quad \frac{1}{g_i} \frac{\partial g_i}{\partial \log h_j} = \frac{h_j}{g_i} \frac{\partial g_j}{\partial h_i}.$$

In this way, the Jacobian is made scale free, and since the relative errors will be commensurate, the two kinds of data will equally influence the correction that improves the current model.

We also show in SIM how the eigenstructure (or singular values) of J may be used to classify the parameters as Irrelevant, Unimportant and Important.

(i) *Irrelevant* parameters have no influence on the model data. They correspond to layers which are out of range of the measurements, or as in the case of thin resistive layers, to parameter combinations that cannot be resolved from the data.

(ii) *Unimportant* parameters have only small influence on model data. Inversely, large changes in these parameters can occur for only marginal improvement in fit to the actual data. For this reason they must be either neglected, or altered only marginally during the inversion process.

(iii) *Important* parameters correspond to the well resolved, and often gross features that are well represented in the data.

Many inverse problems in geophysics are ill-posed. That is, small changes in the data can lead to large changes in the model. The ill-posed nature and consequent numerical instability of the inverse problem is largely contained in its Unimportant and Irrelevant parameters. In SIM we describe an inversion method that filters out the unstabilizing effect on the joint, or separate, inverse problems.

Joint inversion can increase the numbers of Important parameters of a model to include some which the methods cannot resolve separately. It is essential to note that this effect cannot be achieved merely by increasing the number or accuracy of data values of a single method. Rather, joint inversion is a means of eliminating some defects inherent in the individual methods.

To analyse the stability of the result, we have used the Damped Error Bounds described in SIM. These measure the expected variation in the well resolved (Important) parameters, in response to small variations in the data. The bounds ascribed to the Unimportant parameters are damped, and only measure variation due to their correlation with the well resolved parameters. We need to distinguish these narrow limits from the sharp detail of the Important parameters. The greatest 'expected variation' occurs for parameters which are near the 'threshold', or dividing line between the Important, and Unimportant parameters. Usually, these are the most interesting parameters, and the ones most strengthened by combining the two problems.

Example using model data

To see whether joint inversion treats thin layers as anticipated we first studied a three-layer model. The model chosen (Fig. 3) has a thin resistive second layer which is extremely difficult for either method to resolve by itself. The apparent resistivity curves are shown on an expanded linear vertical scale in Fig. 4.

Table 2

Three-layer inversion of three-layer model responses

Inputs: (i) Three-layer model responses (Fig. 4) consisting of MT apparent resistivities at 16 frequencies and Schlumberger (DC) apparent resistivies at 10 electrode spacings, truncated to three figures.

(ii)

	Models	ρ_1	ρ_2	ρ_3	h_1	h_2	RMS error	No. of signif. singular values
	Actual	1	10	1	100	10	—	5
	Starting	1·0	1·0	1·0	50	100		
Outputs:	DC only	1·0	1·9	0·94	89	71	0·2%	4
	MT only	1·0	1·1	1·0	68	82	0·3%	4
	Couple	1·0	9·7	1·0	100	10	0·2%	5

Table 3

Five-layer inversions of three-layer model responses

Inputs:
To 3 (a) Data as to Table 2
To 3 (b) Same data mixed with 3 per cent gaussian error
To 3 (c) Same data mixed with 6 per cent gaussian error.

Models	ρ_1	ρ_2	ρ_3	ρ_4	ρ_5	h_1	h_2	h_3	h_4	RMS error	No. of SSV
Actual	1	10	1	—	—	100	10	∞	—		
Starting	1	1	1	1	1	20	50	50	50		
Outputs											
3 (a) DC	1·0	0·99	1·8	1·6	0·94	23	60	57	50	0·2%	5
MT	1·0	0·97	1·2	1·0	1·0	20	49	51	50	0·3%	5
Coupled	1·0	0·96	5·4	0·78	1·0	40	55	23	28	0·2%	6
3 (b) DC	0·82	1·1	1·9	1·9	0·73	15	86	60	56	1·5%	5
MT	1·6	0·66	2·5	0·75	1·0	19	41	61	47	2·3%	5
Coupled	0·96	0·99	6·0	0·87	1·0	19	70	16	26	2·5%	7
3 (c) DC	1·0	0·97	2·8	2·7	0·47	31	80	60	60	4·3%	4
MT	2·1	0·51	4·3	0·48	0·99	21	33	96	40	4·7%	5
Coupled	1·0	0·89	2·7	0·57	1·0	34	53	83	60	5·0%	7

$\mu = 0{\cdot}01$ (defined in SIM)

DC and MT forward models were calculated. These were variously truncated and mixed with noise, and used as inputs for inversions. Table 2 lists results of the individual inversions and of the coupled inversion, to a 3-layer model, of noise-free data truncated to three figures. These are illustrated in Fig. 5. Five parameters (ρ_1, ρ_2, ρ_3, h_1, h_2) are involved so there are five singular values. Only the four largest are resolved in the individual inversions, as indicated by normalized singular values $+ 0{\cdot}01$ and ρ_2 remains unresolved. The solutions attained show this.

Joint inversion brings all five singular values into the significant range, resolving both ρ_2 and h_2.

In reality, the number of layers present will seldom equal the number in the model chosen for inversion. To study the consequences of an excess of layers in the starting model, the same 3-layer data were inverted to a 5-layer model (9 singular values) with results shown in Table 3(a) and Fig. 6. Here the joint model again did better than the other two, but the resistivity-thickness product is in error by 24 per cent (within the predicted Damped Error Bounds).

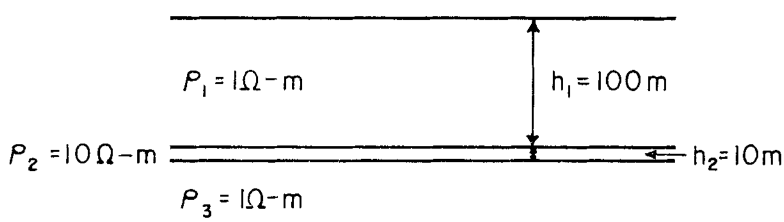

FIG. 3 The model used in the 3-layer inversion study.

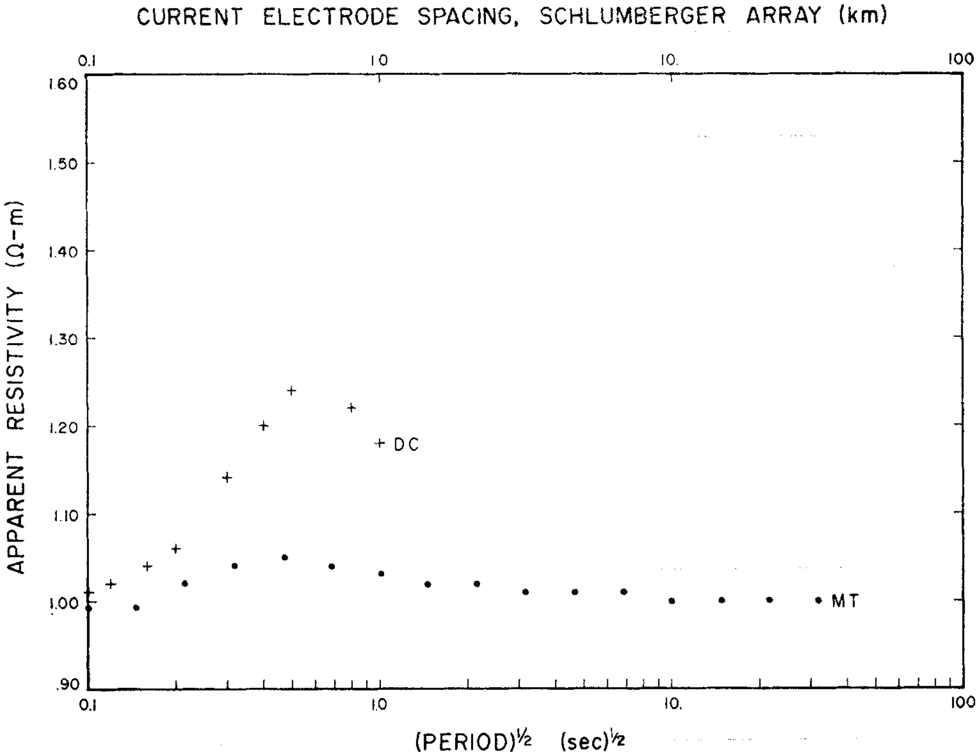

FIG. 4 Input data (truncated) to the 3-layer inversion study.

As a further concession to reality, noise was added to the truncated data before inversion. Gaussian-distributed random noise was added, at levels of 3 and 6 per cent, with results given in Tables 3(b) and 3(c) and Fig. 7. Results deteriorate gradually, but considering the nature of the model it seems remarkable that the results remain as stable as they are.

Additional experiments with changing the lower threshold limit $\bar{\mu}$ (see SIM) made no clear differences.

Field example

DC and MT measurements were made in conjunction with the BMR* at Pirlta, Vic., approximately 50 km WSW of Mildura. The area is in the Murray Basin of New South Wales, South Australia and Victoria. Sparse geophysical and well data indicate that it is comprised of a thin cover of near-horizontal Permian and younger sediments overlying older granites and folded metasediments. The cover may be no more than 1–1½ km thick. Gravity and magnetic coverage is not complete but indicates some lateral contrasts at depths of 2–3 km with a generally north-easterly strike.

Refraction seismic measurements by the Bureau of Mineral Resources (Watson 1962) show a strong refractor at about 0·6 km depth in the Pirlta area. This may be a conglomerate encountered in the only well in the area, AOG Wentworth No. 1, 60 km to the north-east. A later BMR reflection survey obtained coherent primary reflections at nearly 15 s from a 100 kg explosive charge (Branson, Moss & Taylor,

* Bureau of Mineral Resources, Geology and Geophysics, Canberra.

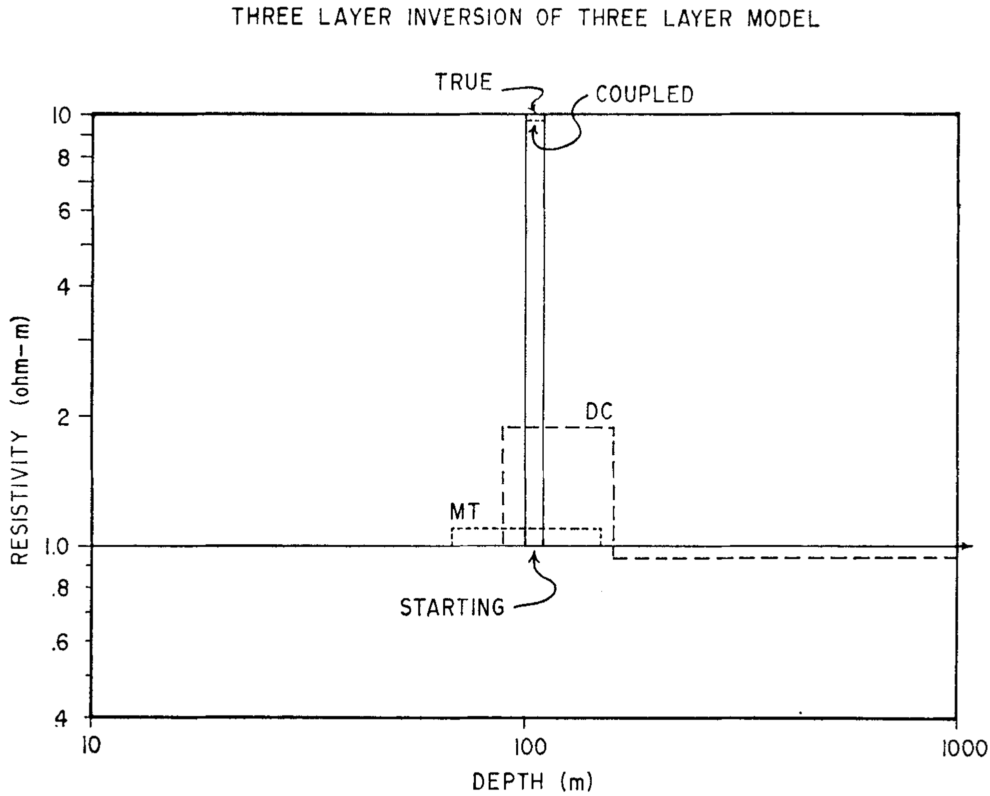

FIG. 5 Result of inverting 3-layer truncated data to a 3-layer model.

1972). Such a remarkable result would seem to indicate minimal scattering and hence simple structural conditions. This is in accordance with the Geomagnetic Depth Sounding results of Lilley & Bennett (1973) which show negligible apparent lateral variation of electrical conductivity at periods of from one minute to one day.

The resulting impression is that the Pirlta area is basically horizontally layered, but with minor lateral variation in magnetic susceptibilities and densities in the 2–5 km depth range.

DC measurements were made along a pair of perpendicular lines crossing at their centers. Schlumberger arrays were used with current electrode spacings from 20 m to 6 km (NS) and 200 m to 6 km (EW). These data together with the inversion results are shown in Fig. 8. A shallow, conductive ($< 1\Omega-$m) shale is widespread, encountered in many water wells (Polak, private communication).

MT measurements were carried out at a site 5 km to the north-west using techniques virtually identical to those described earlier (Vozoff, 1972). Resulting apparent resistivities and principal axis directions are shown in Fig. 9. (For reasons not yet ascertained, data at frequencies above 0·1 hz were unusable.) The major principal axis direction agrees well with the strike direction of the gravity and magnetic data.

When the DC and MT data were jointly inverted the results of Fig. 10 were obtained. Table 4 lists the normalized singular values and their eigenvectors for the final models. These give the interesting result that there is a gap between the second

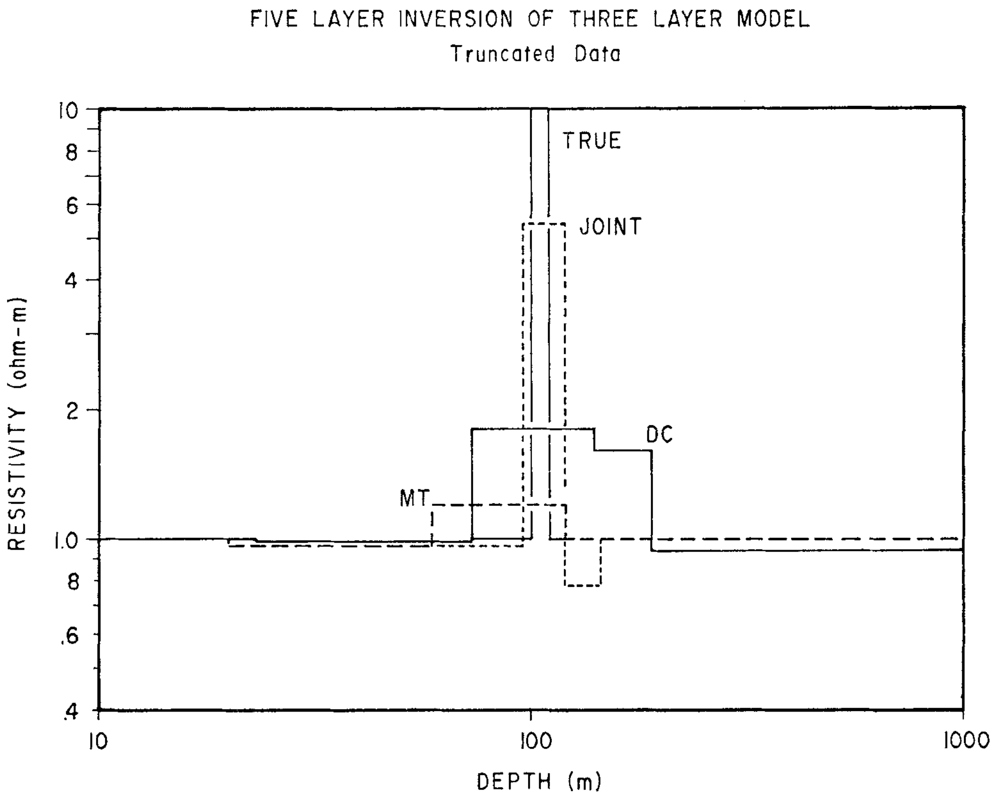

FIG. 6 Result of inverting 3-layer truncated data to a 5-layer model.

and fifth layers, beyond and reach of the DC data but too resistive and shallow for access by most of the MT spectrum. In fact a study of the Jacobian shows that the highest MT frequencies also respond to the shallow conductor but not to layers 3 and 4 beneath it.

That such a situation could arise beneath a thick conductive bed seems reasonable. However, if that depth range happened to be of particular interest, what measurements would help to define its conductivities? Would it help to take DC measurements at larger spacings, or to acquire higher frequency MT data? One way to answer these questions is to examine changes in the list of well-resolved parameters as higher frequencies or larger resistivity electrode spacings are added to the list of measurements. This was done with the major axis MT data set and the EW DC set.

The original data set included ρ_a at 33 frequencies, from $2{\cdot}45\times10^{-3}$ to $7{\cdot}7\times10^{-2}$ hz, and 12 sets of electrode spacings from 200 m to 6 km. We found that extending DC measurements to 26 km had no significant effect on the Damped Error Multipliers. Extending the frequency range upward to 1·0 hz reduced the Damped Error Multipliers for ρ_3, ρ_4, h_3, and h_4, but they remain Unimportant. The conclusion is that, in this configuration of parameters, layers 3 and 4 represent a zone of 'near-blindness' to this combination of measurements.

A number of interesting problems arise in attempting this application. Both DC and MT measurements were made with wires in the N–S and E–W directions. In the normal course of MT analysis it was found that the principal impedance axes at low frequencies were approximately N45E and N45W. Apparent resistivities are computed

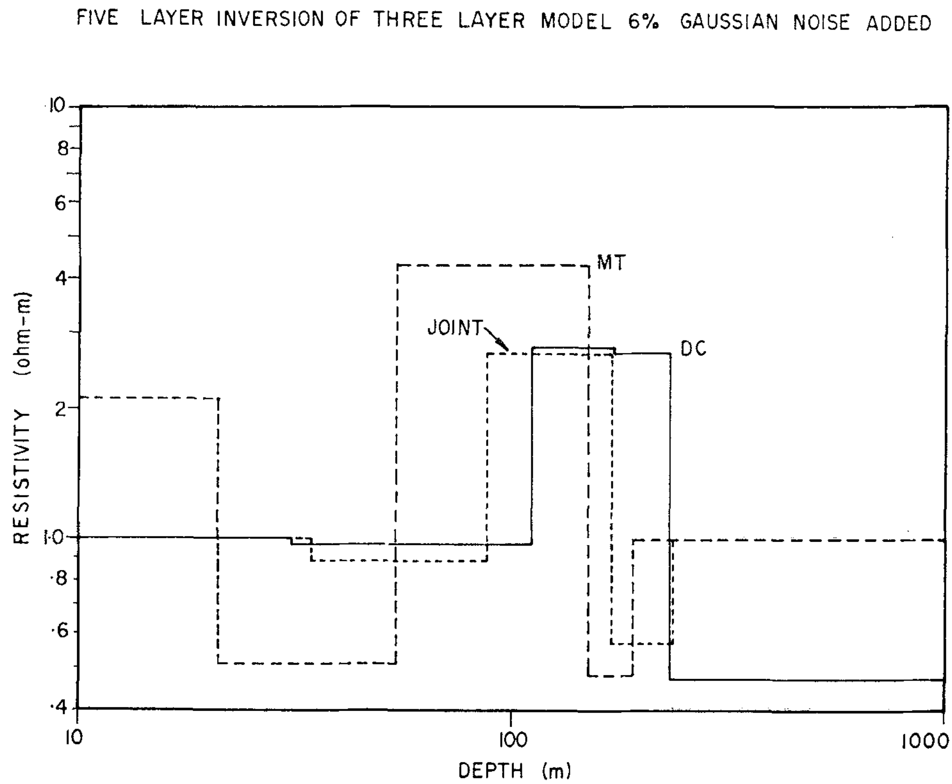

FIG. 7 Result of inverting 3-layer data with 6 per cent error to a 5-layer model.

along principal axis directions. Which DC curves should each be coupled with for joint inversion?

In this particular instance an effort was made to observe possible non-isotropy while making the DC measurements. Potentials were measured perpendicular to the current line at several spacings, but no detectable field was measured in that direction. It was concluded that conditions were isotropic within the depth range of importance to the DC work. There is very little difference between the two DC curves, so that the conclusion could be accepted in this case. Generally it will be necessary to ascertain strike direction, and to make DC measurements in those co-ordinates, if measurements are to be coupled. This will have to be done cautiously, in view of the 'anisotropy paradox' (Maillet 1947) applying to anisotropic media.

Discussion

The examples presented constitute only a preliminary test of the concept. In the field example the data barely overlap in their coverage (because of equipment malfunction), while there is nearly complete coverage by both in the three-layer model studies: one would normally expect a situation somewhere between. Nevertheless they do illustrate the potential of joint inversion to extract the utmost from a method and to define its limits.

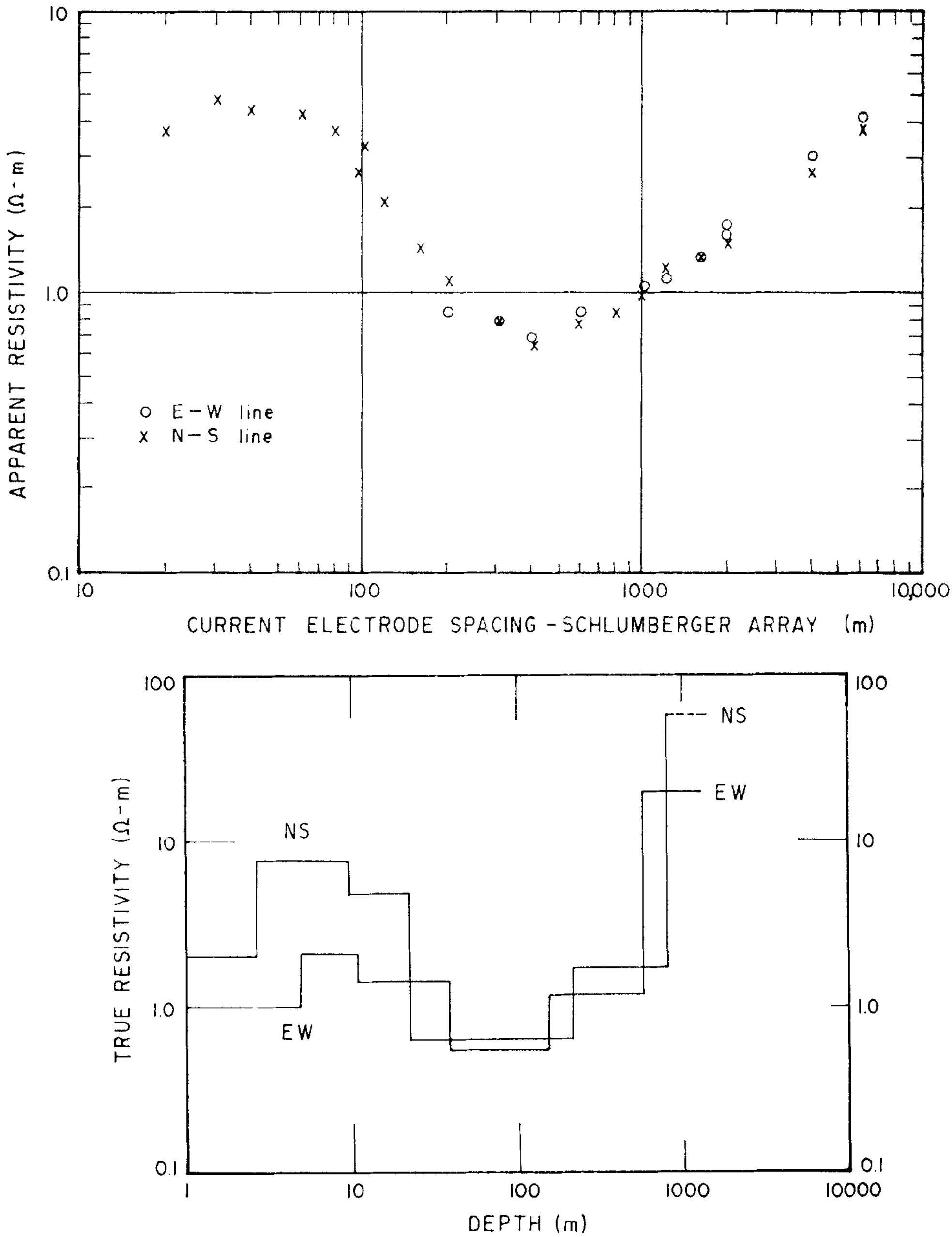

FIG. 8 DC field results at Pirlta, Victoria and results of 6-layer inversion.

Other tests were run on the three layer model to determine the minimum amount of data necessary for a second method to exert a significant effect on the result. It was found that three or four point of DC data were sufficient provided they were well distributed. Ten or twenty extra points had little further effect. This appears to bear out one's intuitive ideas that with noise-free data it is only necessary that the response function be adequately sampled. Field data will always include noise, so there is a good statistical reason to make more than a bare minimum of measurements.

Table 4

Normalized singular values of Jacobian MT major axis/DC E–W

		0·100+01	0·105+00	0·995−01	0·335−01	0·286−02	0·732−03	0·677−03	0·214−03	0·275−04	0·657−05	0·715−17
Parameter space eigenvectors (V matrix)												
ρ_1	1	0·006	−0·022	0·025	0·150	−0·084	0·914	0·214	−0·295	0·024	−0·006	0·006
ρ_2	2	0·716	−0·474	0·458	−0·229	0·008	0·008	−0·002	−0·005	0·000	−0·000	0·000
ρ_3	3	0·060	0·039	−0·043	0·022	0·011	−0·056	−0·009	−0·153	0·060	−0·033	0·980
ρ_4	4	0·004	0·003	−0·003	0·002	0·015	−0·046	−0·005	−0·165	0·065	0·983	0·000
ρ_5	5	0·013	0·017	−0·010	0·023	0·990	0·080	0·102	0·051	0·004	−0·002	−0·000
ρ_6	6	−0·001	−0·004	−0·003	−0·001	−0·082	−0·227	0·970	0·021	0·003	−0·001	0·000
h_1	7	−0·002	−0·222	0·243	0·932	−0·003	−0·141	−0·033	0·050	−0·004	0·001	−0·001
h_2	8	−0·691	−0·447	0·501	−0·235	0·034	−0·011	0·001	−0·096	0·032	−0·013	0·069
h_3	9	−0·059	−0·040	0·045	−0·026	0·065	0·270	0·041	0·848	−0·358	0·180	0·184
h_4	10	−0·004	−0·001	0·005	−0·003	0·030	0·087	0·008	0·359	0·929	0·004	0·005
h_5	11	0·035	0·723	0·690	−0·007	−0·006	−0·002	0·004	−0·002	−0·002	−0·000	−0·001

Normalized singular values of Jacobian MT minor axis/DC N–S

		0·100+01	0·419−00	0·307−00	0·149−00	0·108+00	0·291−02	0·173−03	0·104−03	0·725−05	0·569−05	0·148−05
Parameter space eigenvector (V matrix)												
ρ_1	1	0·013	−0·017	0·660	0·642	0·390	−0·000	0·000	−0·000	0·000	0·000	−0·000
ρ_2	2	0·740	−0·110	0·115	−0·434	0·489	−0·001	0·001	−0·000	0·000	0·000	−0·000
ρ_3	3	0·040	−0·004	−0·010	0·029	−0·033	−0·001	0·080	−0·090	0·991	−0·001	−0·019
ρ_4	4	0·002	−0·000	−0·001	0·002	−0·002	−0·000	0·062	−0·147	0·000	0·000	0·987
ρ_5	5	0·001	−0·000	−0·000	0·001	−0·002	−0·011	0·941	0·335	−0·046	0·017	−0·009
ρ_6	6	−0·000	0·012	0·001	−0·002	0·003	1·000	0·011	0·003	0·000	0·001	−0·000
h_1	7	0·016	−0·023	0·723	−0·405	−0·559	0·000	−0·000	0·000	−0·000	−0·000	0·000
h_2	8	−0·651	0·116	0·166	−0·484	0·542	−0·004	0·025	−0·058	0·053	0·019	−0·006
h_3	9	−0·038	0·012	0·010	−0·029	0·033	0·001	−0·291	0·857	0·107	−0·380	0·146
h_4	10	0·001	0·020	0·001	−0·002	0·002	−0·000	−0·138	0·347	0·045	0·924	0·060
h_5	11	0·161	0·986	0·022	0·010	−0·016	−0·011	0·004	−0·011	−0·005	−0·017	−0·002

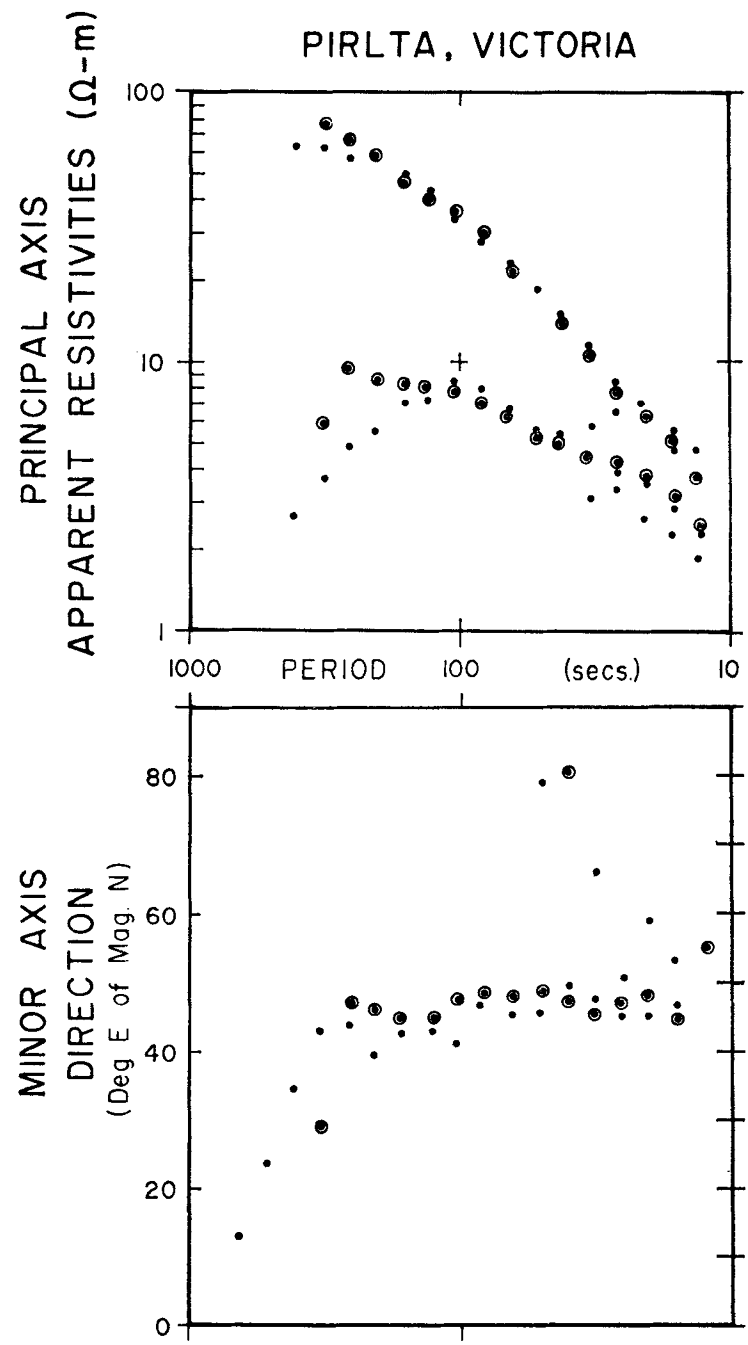

FIG. 9 MT field results at Pirlta, Victoria. Rotated tensor (principal axis) resistivities and principal axis direction.

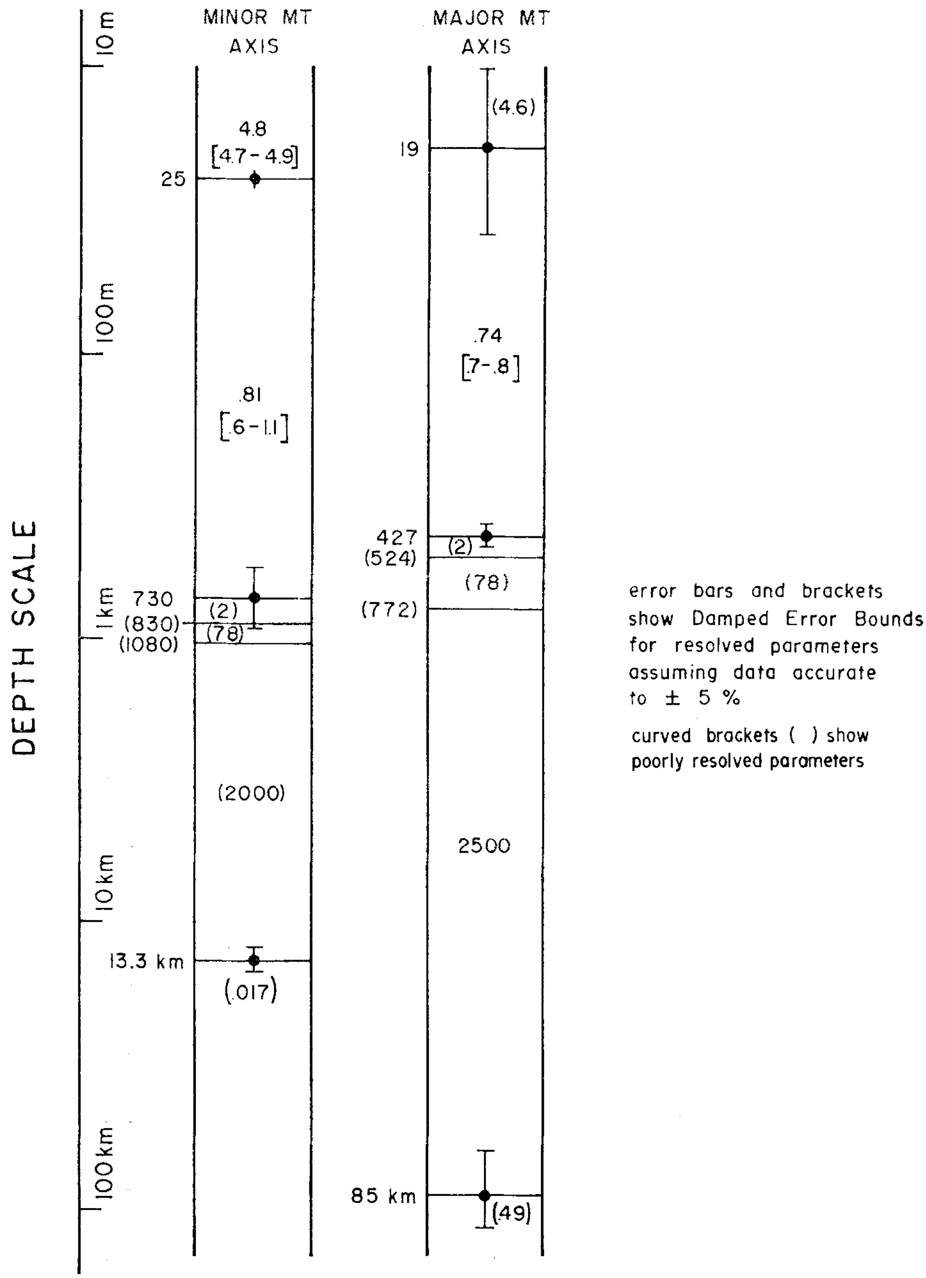

FIG. 10 Results of joint inversions to layered models, Pirlta, Victoria.

Joint inversion has some implications for the design of measurement programs. The location of new measurements for greatest effectiveness depends on a very non-linear way on the true conductivity distribution. If each measurement is expensive then one would make a few, invert, and (from the result) find the best parameters for the next set of measurements, etc. In geophysics it is often more expensive to return to a site than to take extra measurements, so that an excess of measurements is made to start. However there are clearly some situations when the reverse is true.

There exists an unavoidable influence of the starting model on the final model. It appears to be less with the present strategy than with many earlier approaches, and the Damped Error Bounds appear to accurately define the tolerance ranges for significant parameters.

Extending joint inversion to include other kinds of electrical or electromagnetic measurements can be done in the same way as we have done here. It would be equally interesting to include indicators of other physical properties—seismic surface wave characteristics for example—but their incorporation within a common framework will require further study.

Acknowledgments

The Australian Research Grants Committee and Macquarie University supported this research. The Bureau of Mineral Resources, Geology and Geophysics made it possible to acquire the field data. In particular Mr D. Kerr and Dr E. Polak of the BMR and Dr R. J. G. Lewis of Macquarie University (now at the University of Tasmania) made major contributions to the collection and analysis of the data. We are also indebted to Dr Jack Cribb of the CSR Research Department and Dr David Johnson of Macquarie University for their critical comments.

References

Branson, J. C., Moss, F. J. & Taylor, F. J., 1972: Deep Crustal Reflection Seismic Test Survey, Mildura, Victoria and Broken Hill, N.S.W. *Bureau of Mineral Resources Record* 1972/127, Canberra.

Inman, J. R., Ryu, J. & Ward, S. H., 1973: Resistivity inversion, *Geophysics*, **38**, (6), 1088–1108.

Jupp, D. L. B. & Vozoff, K., 1975. Stable iterative methods for the inversion of geophysical data, *Geophys. J. R. astr. Soc.* **42**, 957–976

Kowalik, J. & Osborne, M. R., 1968. *Methods for unconstrained optimization problems*, American Elsevier.

Lilley, F. E. M. & Bennett, D. J., 1973. Micropulsations recorded by an array of magnetic variometers, *J. geophys. Res.*, **78**, (10), 1603–1607.

Madden, T. R., 1972. Transmission systems and network analogies to geophysical forward and inverse problems. *Tech. Report No.* 72–3, Department of Earth Sciences, MIT, 45 pp.

Maillett, R., 1947. The fundamental equations of electrical prospecting, *Geophysics*, **12**, (4), 529–556.

Parker, R. L., 1970. The inverse problem of electrical conductivity in the mantle, *Geophys. J. R. astr. Soc.*, **22**, 121–138.

Vozoff, K., 1972. The magnetotelluric method in the exploration of sedimentary basins, *Geophysics*, **37**, (1), 98–141.

Ward, S. H., 1967. Electromagnetic theory for geophysical applications, in *Mining Geophysics*, v.2, Society Exploration Geophysics, Tulsa.

Watson, S. J., 1962. Murray Basin Seismic Survey, 1960, *Bureau of Mineral Resources Record No.* 1962/164, Canberra, 19 pp.